Synthesis and Photophysical Evaluation of 3,3'-Nitrogen Bis-Substituted fac-[Re(CO)₃(Diimine)Br] Complexes

Csucker, Joshua ; Decrausaz, Nathalie ; Jäggi, Sarah Isabella ; Blacque, Olivier ; Spingler, Bernhard ; Alberto, Roger

DOI: https://doi.org/10.1002/hlca.202300239

doi.org/10.1002/hlca.202300239

RESEARCH ARTICLE

HELVETICA chimica acta

Synthesis and Photophysical Evaluation of 3,3′-Nitrogen Bis-Substituted *fac*-[Re(CO)$_3$(Diimine)Br] Complexes

Joshua Csucker[+],*[a] Nathalie Decrausaz[+],[a] Sarah Isabella Jäggi,[a] Olivier Blacque,[a] Bernhard Spingler,[a] and Roger Alberto*[a]

[a] Department of Chemistry, University of Zurich, Winterthurerstrasse 190, 8057 Zürich, Switzerland, e-mail: joshua.csucker@chem.uzh.ch; ariel@chem.uzh.ch

The preparations, photophysical and electrochemical properties of a series of *fac*-[Re(CO)$_3$(diimine)Br] complexes are presented. The bipyridine (bpy) based diimine ligands feature symmetrical and asymmetrical 3,3′-diamino-2,2′-bipyridine substitution patterns. Photophysical and electrochemical properties of these complexes are tunable, depending on their organic diimine framework. Introduction of a distal urea bridge *via* the 3,3′-substitution pattern led to prolonged phosphorescence lifetimes without a significant change in absorbance and phosphorescence emission wavelengths. Reversible electrochemical bipyridine reduction remained largely unchanged by this derivatization.

Keywords: Bipyridine, Cyclic Voltammetry, Fluorescence, Ligand Design, Phosphorescence, Rhenium Tricarbonyl, Synthesis.

Introduction

Fac-[Re(CO)$_3$(diimine)X] (X = halide) complexes are a staple class of catalysts in homogeneous CO_2 to CO reduction. The diimine ligands are typically bipyridine (bpy) derivatives due to the favorable photo- and electrochemical properties of *fac*-[Re(CO)$_3$(bpy)Br] complexes. Namely, these complexes are strongly absorbing in the lower visible range of the solar spectrum with phosphorescence emissions in the orange to red part.[1–5] Excited states are long-lived[6] showing no loss of carbonyl or diimine ligands.[7–10] As a result, electrochemical[11,12] and photocatalytic[13,14] CO_2 to CO reduction procedures have been established *in tandem* in the mid-eighties already by e.g. the Ziessel group.[15,16] Furthermore our group has applied *fac*- [Re(CO)$_3$(diimine)X] complexes as photosensitizers in photocatalytic water to hydrogen reduction.[2,3,5] Generally, *fac*-[Re(CO)$_3$(diimine)X] complexes rely on three main derivatization strategies for system optimization. Modification of the diimine ligand allows tailoring of the photophysical behavior of the complex, since the LUMO is largely located on the diimine ligand.[4,17,18] The HOMO, on the other hand, is generally impacted by the rhenium d-orbitals and the carbonyl ligands. Finally, substitution of the axial halide by a neutral ligand leads to water soluble [Re(CO)$_3$(diimine)L]$^+$ complexes.[17] Strong field ligands like thiocyanate suppress ligand exchange with solvents.[2–4,19]

We were particularly interested in 3,3′-nitrogen bis-substituted bipyridines as chelators. The inherent steric clash between the substituents is the reason why the 3,3′-substitution pattern is often overlooked in lieu of 5,5′- or 6,6′-systems. We were inspired by the proximity of the two substituents. Amino and nitro 3,3′-bis-substituted bipyridyl chelators have been reported.[20,21] We envisaged to exploit the proximity of the amino groups and introduce fused 6-6-6 and 6-7-6 membered diimine chelators.[22] The diamine motif would serve as chemical handle to create fused 6-7-6 membered bipyridyl derivatives. Specifically, we aimed to bridge the amines with urea, thiourea and an sp^2

[+] These authors contributed equally

Supporting information for this article is available on the WWW under https://doi.org/10.1002/hlca.202300239

hybridized carbon to investigate the effect of these groups on the electrochemical and photophysical properties of the resulting *fac*-$\{Re(CO)_3\}^+$ complexes. Electron donating amines and derivatives thereof should make the complexes stronger reducing agents if they act as photosensitizers.

Results and Discussion

We prepared seven 3,3′-*N*-substituted-bipyridine chelators starting from 3,3′-dinitro 2,2′-bipyridine **1** (*Scheme 1*). Treatment of **1** with sodium sulfide in water gave a fused 6-6-6 membered azaphenanthrene chelator **2**. Reacting **1** with $SnCl_2$ in aqueous HCl reduced the nitro-groups to the respective amines and provided compound **3**. These diimine chelators can be purified by either SiO_2 flash column chromatography or reverse phase preparative HPLC (see ESI for details). Analytical data of **1**–**3** were consistent with the literature.[1,20,21,23]

Seven-membered rings were introduced on the bipyridyl framework starting from **3**. Following a procedure reported by Matsuda *et al.*, condensation of **3** with benzimidate provided compound **4**.[21] This chelator was coordinated *in situ* to the *fac*-$\{Re(CO)_3\}^+$ core (*vide infra*). To obtain urea- and thiourea-bridged 3,3′-N-substituted bipyridyls, compound **3** was reacted with urea in acetic acid, providing the urea-bridged bipyridyl **5** in good yields (64%). More reactive carbonylation reagents such as chloroethyl formate and triphosgene were also explored but they were less effective at producing **5** compared to urea with lower yields and requiring longer reaction times. Treatment of **3** with CS_2 in DMSO gave the thiourea compound **7** in quantitative yields. Analogous reactions with CO_2 as carbonyl source showed no conversion of **3**.

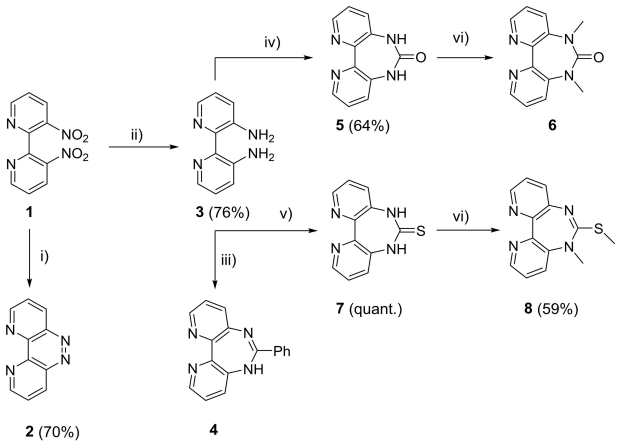

Scheme 1. Reaction conditions: i) $Na_2S \cdot H_2O$, H_2O/MeOH 15:1, 16 h, r.t.; ii) $SnCl_2$, conc. HCl, EtOH, 5 h 70 °C; iii) benzimidate hydrochloride, EtOH, 1.5 h, 80 °C; iv) urea, AcOH, 3 h, 120 °C; v) CS_2, DMSO, 45 min, 120 °C; vi) KOH, MeI, DMSO, r.t, 6.5 h.

Methylation of **5** and **7** with methyl iodide in DMSO produced the bis-methylated compounds **6** and **8** respectively. The differences in chemoselectivities of the methylation reaction between the urea and the thiourea groups is remarkable. Both nitrogen atoms of **6** were methylated while its thiourea congener **8** was methylated on the sulfur and one nitrogen atom resulting in an en-thiol like 7-membered ring. Evidently, the thiol-thione tautomerization was shifted towards the thiol by the alkaline methylation conditions. This tautomer is methylated more easily due to the high nucleophilicity of the thiol.[24] Compound **6** was not isolated due to its strong hygroscopic nature. Direct coordination to the *fac*-$\{Re(CO)_3\}^+$ core gave the respective *fac*-[$Re(CO)_3$(diimine)Br] complex in good yields (*vide infra*). Methylation of **4** is possible, however, Fairful *et al.* report that the resulting product is very susceptible towards nucleophilic attack and hydrolysis.[25] Attempts to obtain an *N*-methyl derivative of **4** yielded either the hydrolysis product or **10** after isolation or direct complexation.

All bipyridyls **4**–**8** were analyzed by standard analytical techniques (NMR, IR, HR-ESI-MS, elemental analysis, see ESI for details). Single crystal XRD analysis of **5**, **7**, **8** unambiguously assessed their chemical structures. Crystallographic data are provided in the electronic supporting information (*Tables S1–4*). A common feature of the diimines are their twisted structures. The strain imposed by the fused 6-7-6 ring system distorts the molecular geometry and induced a twist along the pyridine-pyridine C–C bond. All *fac*-[$Re(CO)_3$(diimine)Br] complexes in this work were synthesized with a standardized method. The bipyridines **1**–**8** were added to a degassed solution of $(NEt_4)_2[Re(CO)_3Br_3]$ in refluxing methanol. The brightly colored [$Re(CO)_3$(diimine)Br] complexes precipitated from the reaction solutions either directly or upon cooling (*Scheme 2*). Thus, the reaction progress can even be followed by eye. Alternatively, an aliquot of the reaction can be filtered, and the filtrate checked by FT-IR or UHPLC-MS. *Fac*-$\{Re(CO)_3\}^+$ complexes exhibit a sharp band around 2020 cm^{-1} for the asymmetric and a broad band at 1900 cm^{-1} for the two symmetric $\nu(C\equiv O)$ stretching modes (*Table 1*).

The products were collected by filtration and washed with cold ethanol. All *fac*-[$Re(CO)_3$(diimine)Br] complexes **9**–**15** were obtained in good yields. Their structures were confirmed by standard analytical

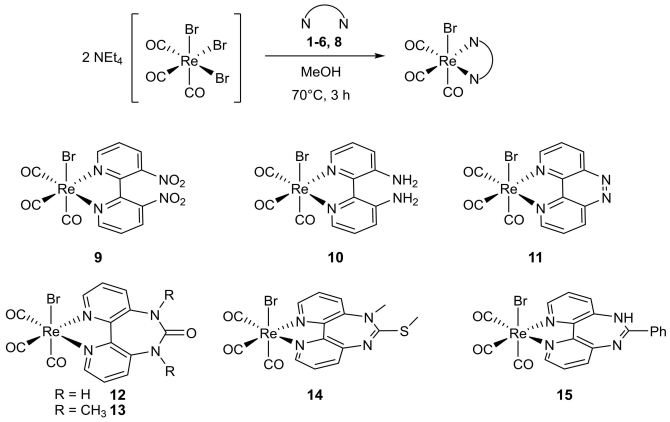

Scheme 2. Standard reaction conditions for the complexation of 3,3′-*N*-substituted bipyridines.

techniques (NMR, FT-IR, HR-ESI-MS, elemental analysis) as well as single crystal X-ray diffraction analysis (see ESI).

Complexation reactions can be performed at milligram to gram scale without noticeable differences in yields. In principle, **4** may also chelate the *fac*-{Re(CO)$_3$}$^+$ core via one or both of the amines.[23] No evidence for such a coordination mode was observed in either ^{1}H-NMR or FT-IR.

Structural comparisons of the novel *fac*-[Re(CO)$_3$(diimine)Br] complexes is based on their single crystal X-ray analyses (*Figure 1*). The bipyridyl ligand of **12** is twisted while **13**–**15** show asymmetrically distorted diimine frameworks. No distortion of the seven membered rings **12** and **13** was observed in solution on NMR time scale. All N–Re–N bite angles are around 74.5° with small deviations (see *Table 1*). Other common features are the slightly distorted C–Re–Br angles deviating from the ideal 180° by between 3 and 7°. A comprehensive overview of all relevant crystallographic data is provided in the electronic supporting information (*Tables S5*–*16*).

Application of the standard reaction conditions of (NEt$_4$)$_2$[Re(CO)$_3$Br$_3$] with the thiourea **7** did not result in a classical *fac*-[Re(CO)$_3$(diimine)Br] complex (*Scheme 3*). Instead, the anionic bimetallic species NEt$_4$**[16]** was obtained in 57% yield. NEt$_4$**[16]** shows two sets of characteristic ν(C≡O) stretching bands in the FT-IR. The bands at 2022 and 1910 cm^{-1} were assigned to the *fac*-[Re(CO)$_3$(diimine)Br] fragment and those at 2009 and 1892 cm^{-1} to the [Re(CO)$_3$Br$_2$S]$^-$ fragment. Single crystal XRD determination confirmed the structure unambiguously. The N–Re–N bite angle was in line with those of **9**–**15** with 74.5(2)°. The *fac*-{Re(CO)$_3$}$^+$ core is known to react rapidly with thiols and thiones.[28,29]

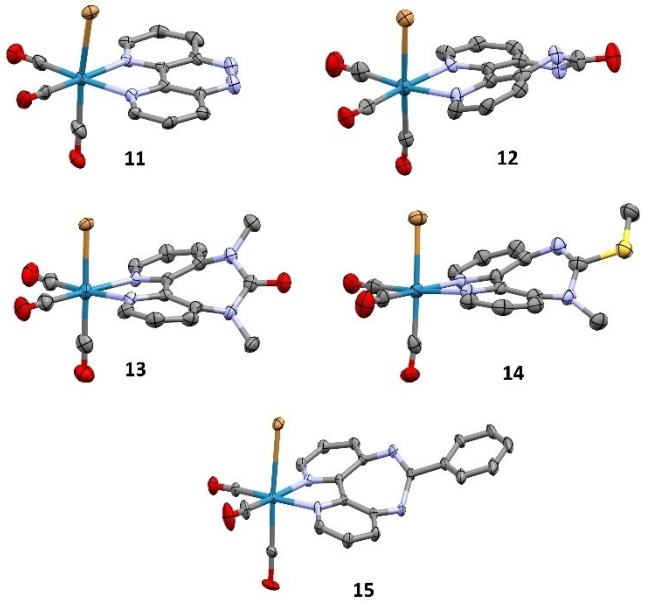

Figure 1. Ellipsoid displacement plots[27] of **11** (top left), **12** (top right), **13** (middle left), **14** (middle right) and **15** (bottom). Hydrogen atoms and counter ions were omitted for clarity. Thermal ellipsoids represent 50% probability.

Table 1. Yields, C≡O stretching frequencies and bite angles of **9**–**15**.

Compound	Yield [%]	νCO [cm^{-1}]	N–Re–N angle [°]
9	63	2031, 1921	–
10	78	2030, 1900	–
11	>99	2024, 1901	76.6(1)
12	67	2022, 1901	74.7(3)
13	17[a]	2022,1926	74.2(2)
14	38	2024,1906	74.2(2)
15	58[a]	2020,1899	74.85(6)
[Re(CO)$_3$(bpy)Br][b]	91	2019, 1905	74.7(4)

[a] Yield over two steps, based on **3**, [b] data from literature[26].

Thus, we assessed that the sulfur atom in **7** coordinates to the first equivalent of *fac*-[Re(CO)$_3$Br$_3$]$^{2-}$ under kinetic control. Chelation of a second equivalent completes the reaction. Formation of bimetallic complexes was omitted by methylating the chelator to the respective methyl-thioether **8** as mentioned above.

We evaluated the electrochemical and photophysical properties of **9**-**[16]**$^-$ to establish the influence of the distorted chelators on the rhenium center. The standard complex [Re(CO)$_3$(bpy)Br] has two main reduction waves in cyclic voltammetry; reversible

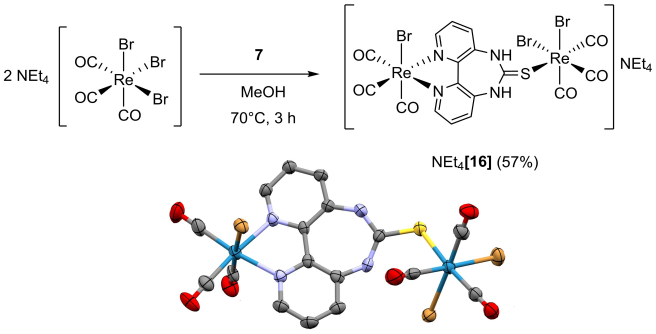

Scheme 3. Reactions of $(NEt_4)_2[Re(CO)_3Br_3]$ with **7** yielded a dimeric structure with two *fac*-$\{Re(CO)_3\}^+$ units bridged by **7** via the bipyridyl and the sulfur of the thiourea bridge. Bottom: Ellipsoid displacement plot[27] of **[16]**$^-$ of the crystal structure NEt_4**[16]**. Hydrogen atoms and counter ions were omitted for clarity. Thermal ellipsoids represent 50% probability.

$bpy^{0/-I}$ ($E_{1/2} = -1.74$ V) and irreversible $bpy^{-I/-II}$ ($E_{red} = -2.15$ V) reductions versus Fc/Fc+.[10] Cyclic voltammetry was recorded of **10**-NEt_4**[16]** in DMF (*Table 2*). Complex **9** decomposes quickly in DMF hence corresponding data are not included. The cyclic voltammogram of **10** showed no reversible reduction process. Instead, an irreversible two electron reduction at −2.02 V was observed. Increasing the scan rates from the standard 0.5 V/s to 1 V/s did not contribute additional information. In contrast to $[Re(CO)_3(bpy)Br]$, the azaphenantroline complex **11** showed four reduction processes. The reversible $bpy^{0/-I}$ reduction at −1.077 V. was strongly anodically shifted whereas the irreversible $bpy^{-I/-II}$ reduction at $E_{red} = -2.21$ V was slightly cathodically shifted compared to $[Re(CO)_3(bpy)Br]$. Two additional irreversible reduction waves were observed at −1.89 V and −2.44 V, likely originating from stepwise reduction of the diazo moiety.

Complexes with the fused 6-7-6 membered diimine chelators (**12**-**[16]**$^-$) behave very similar to $[Re(CO)_3(bpy)Br]$ albeit with cathodically shifted reduction potentials throughout. The urea bridged complex **12** displayed the lowest $E_{1/2}$ $bpy^{0/-I}$ potential (−1.73 V) while the dinuclear complex NEt_4**[16]** the highest one (−1.55 V). The urea- and thiourea-bridged complexes **12** and **[16]**$^-$ varied only slightly in their electrochemical behavior pointing towards negligible similar inductive effects between thiourea and urea functionalities. The carbon bridged complex **15** had higher $bpy^{0/-I}$ reduction at −1.60 V (+0.13 V *versus* **12**). Methylation slightly shifted $bpy^{0/-I}$ reduction potentials anodically compared to their unmethylated counterparts. The reversible $E_{1/2}$ $bpy^{0/-I}$ reduction of **13** ($E = -1.64$ V) was only 0.07 V lower than **12**.

Evidently, the introduction of nitrogen substituents at the 3,3′ position led to a slight cathodic sift of $E_{1/2}$ $bpy^{0/-}$ potentials due to electron donating effects. The overall electrochemical behavior of *fac*-$[Re(CO)_3(bpy)Br]$ remains largely unchanged by the introduction of fused 6-7-6 diimine ligands. Methylation does not significantly affect the electrochemistry of the *fac*-$[Re(CO)_3(diimine)Br]$ complexes.

Absorbance and emission spectra of compounds **10**-**[16]**$^-$ were recorded in DMF. The lowest HOMO-LUMO transitions in *fac*-$[Re(CO)_3(diimine)Br]$ systems are assigned to metal to ligand charge transfers (MLCT).[30] All complexes except **15** ($\lambda_{max} = 362$ nm) showed MLCT absorbance maxima either at or above that of $[Re(CO)_3(bpy)Br]$ ($\lambda_{max} = 375$ nm).[26] The electron donating substituents on the diimines, leading to stabilization of the LUMO located on the ligand

Table 2. Summary of the photo- and electrochemical data of compounds **9**-**[16]**$^-$ in DMF.

Compound	τ [ns]	λ_{max} MLCT [nm]	ε [$M^{-1}\cdot cm^{-1}$]	λ_{em} [nm]	$E_{1/2}$ $bpy^{0/-I}$ [V]
9	_[a]	_[a]		_[a]	_[a]
10	0.9 ± 0.1	514	1640	618 (P)	_[b]
11	9.3 ± 0.1	397	4152	453 (F)	−1.08
12	81.2 ± 1.3	387	8848	643 (P)	−1.73
13	26.3 ± 0.1	374	8795	655 (P)	−1.64
14	9.8 ± 0.1	395	4447	453 (F)	−1.66
15	1.5 ± 0.1, 5.2 ± 0.3, 23.4 ± 3.8	362	8916	501 (F), 541 (F), 609 (P)	−1.60
NEt_4[**16**]	73.7 ± 0.7	412	7937	662 (P)	−1.55
$[Re(CO)_3(bpy)Br]$	49.3 ± 0.2	375	3291	620 (P)	−1.77

All photophysical measurements were performed in degassed solutions at 25 μM analyte concentration. Emissions are classified into phosphorescence (P) and fluorescence (F). Conditions for cyclic voltammetry: 1 mM analyte concentration with 0.1 M $TBAPF_6$ in DMF as electrolyte, scan rate was 0.5 V/s in 0.005 V steps. Potentials were calibrated *versus* the $[Fe(C_5H_5)_2]/[Fe(C_5H_5)_2]^+$ redox couple. [a] Compound is not stable in DMF. [b] No reversible reduction observed.

framework, explain red-shift trends.[17,18] This effect was strongest for **10** ($\lambda_{max} = 514$ nm) exhibiting strong batochroism. An additional absorbance at 487 nm was observed for **15**. The compounds were further classified into three groups according to their molar extinction coefficients (ε). MLCT transitions with strong absorbers (**12**, **13** and **15**) generally absorb with $\varepsilon > 8500\ M^{-1}\cdot cm^{-1}$ while ε values of **11** and **14** are substantially lower. Only **10** was weakly absorbing with $\varepsilon = 1640\ M^{-1}\cdot cm^{-1}$. As a reference, the ε value of *fac*-[Re(CO)$_3$(bpy)Br] is 3300 $M^{-1}\cdot cm^{-1}$.

Phosphorescence dominates the emission features of *fac*- [Re(CO)$_3$(diimine)Br] complexes and for all compounds presented herein. Emission wavelengths (λ_{em}) were broad with maxima >600 nm (*Table 2*), reflecting their bright orange to red colors. For compounds **11** and **14** only fluorescence emission was detected. Recording luminescence of **14** in THF showed a fluorescence ($\lambda_{max} = 456$ nm) and phosphorescence ($\lambda_{max} = 650$ nm). Thus, strong solvent interactions with DMF may suppress intersystem crossing and the resulting phosphorescence. Compound **15** showed two distinct fluorescence bands in addition to phosphorescence.

Potential photosensitizers require excited state lifetimes $\tau > 20$ ns to efficiently act as electron transfer agents after reductive quenching.[26] The phosphorescence lifetime of **10** is clearly too short for this purpose with only 0.9 ± 0.1 ns. The primary emissive transition of **11** was fluorescence with a lifetime of 9.3 ± 0.1 ns. Restricting the degrees of freedom by bridging the amines extended the excited state lifetimes significantly. The urea bridged complex **12** had the longest phosphorescence lifetime of this series with 81.2 ± 1.3 ns. The respective species with the thiourea-bridged diimine NEt_4**[16]** showed a phosphorescence lifetime of 73.7 ± 0.67 ns. Phosphorescence lifetime of **15** was 23.4 ± 3.8 ns while its two fluorescence emissions were short-lived (1.5 ± 0.1, 5.2 ± 0.3 ns). Methylation led to faster excited-state relaxation, presumably through the reintroduction of rotational degrees of freedom. Complex **13** ($\tau = 26.3 \pm 0.1$ ns) displayed a significantly shorter-lived phosphorescence state compared to **12**. The influence of methylation was more pronounced with **14**. In contrast to NEt_4**[16]**, only fluorescence emission was observed with **14** ($\tau = 9.8 \pm 0.1$ ns). A strong phosphorescence with λ_{em} at 650 nm was observed when recording emission in THF. The lifetime of 45.9 ± 0.7 ns was shorter than the non-methylated NEt_4**[16]**.

Evidently, the newly prepared diimine chelators **4**, **5** and **7** stabilize excited states in respective *fac*-[Re(CO)$_3$(diimine)Br] complexes. Phosphorescence lifetimes extended but the absorbance maxima red-shifted only marginally compared to *fac*-[Re(CO)$_3$(bpy)Br]. Specifically, the urea bridged chelator appears to induce favorable photo- and electrochemical properties for potential applications as photosensitizer.

Conclusions

A series of new 3,3′-*N*-substituted bipyridyl chelators and their *fac*-[Re(CO)$_3$(diimine)Br] complexes is reported. The substitution motif influenced the reduction potentials, absorbance and emission wavelengths and excited state lifetimes of the respective *fac*-{Re(CO)$_3$Br} complexes. Finetuning of these characteristics can be achieved by controlling the oxidation state of the nitrogen substituents or by choosing fused 6-7-6 ring diimine chelators. Along this line, complexes with absorption maxima spanning a range from the UV into the visible spectrum (370 to 515 nm) were obtained. Equally, reversible $bpy^{0/-I}$ reduction potentials between −1.55 and −1.729 V were observed. As such, the presented *fac*-[Re(CO)$_3$(diimine)Br] complexes with fused 6-7-6 ring diimine chelators have similar electrochemical behavior as *fac*-[Re(CO)$_3$(bpy)Br]. Merely **11** showed a fundamentally altered electrochemical behavior with an irreversible two electron reduction process instead of reversible $bpy^{0/-I}$ reduction. Urea bridged systems possess the longest lifetimes with about two-fold longer-lived phosphorescence compared to *fac*-[Re(CO)$_3$(bpy)Br]. These factors combine in **12** to make it a promising new photosensitizer. Therefore, derivatizations of the functionalities in the 3,3′-positions of the 2,2′-bipyridyl system enable excellent tunabilities of individual photo- and electrochemical properties. Thereby, the long known *fac*-[Re(CO)$_3$(diimine)Br] core and its previously known derivatives can be complemented for more tailor-made photosensitizers and catalysts.

Experimental Section

General Methods and Material

Chemicals and solvents: All chemicals were of reagent grade or higher, obtained from commercial sources (*Fluorochem*, *Alpha Aesar*, *Merck*, *Fluka* and *Fisher Scientific*) and used without further purification. Solvents were of p.a. grade or distilled prior to their use; H_2O was bidistilled. Deuterated NMR-solvents were

purchased from *Armar Chemicals* or *Cambridge Isotope Laboratories, Inc. (UK)*. PH indicators were *Merck* indicator paper pH 1–14 (universal indicator). ^{1}H- and ^{13}C-NMR: *Bruker AV2-400* (400 MHz) or *Bruker AV2-500* (500 MHz); in deuterated solvents at 300 K; chemical shifts (δ) in ppm relative to residual solvent resonances ($CDCl_3$ ^{1}H: δ 7.26, 13 C: δ 77.16; MeOD-d_4 ^{1}H: δ 3.31, ^{13}C: δ 49.00; THF-d_8 ^{1}H: δ 3.58, δ 1.72, 13 C: δ 67.21, δ 25.31; DMSO-d_6 ^{1}H: δ 2.50, ^{13}C: δ 39.52); coupling constants (J) in Hz. Signal assignments are based on coupling constants, increment calculations and/or 2D-NMR experiments. FT-IR spectra: *SpectrumTwo* FT-IR Spectrometer (*Perkin-Elmer*) equipped with a *Specac Golden GateTM* ATR (attenuated total reflection) accessory; applied as neat samples; 1/λ in cm^{-1}. Where *s* = strong, *m* = medium, *w* = weak signals. Specific information to UHPLC-MS, HR-ESI-MS, preparative HPLC X-Ray diffraction measurements, UV-Vis, excited state lifetime and emission measurements as well as cyclic voltammetry are listed in chapter 1 of the electronic supporting information.

Diimine Syntheses

5,7-Dihydro-6H-dipyrido[3,2-d:2′,3′-f][1,3]diazepin-6-one (5)

Adapted from literature.[31] Compound **3** (300.0 mg, 1.61 mmol, 1.0 eq.) and urea (242.0 mg, 4.02 mmol, 2.5 eq.) were dissolved in glacial acetic acid (3 mL) and heated to 120 °C for 3 h, until UHPLC-MS indicated full consumption of the starting material. After the reaction mixture was cooled to ambient temperature, THF (20 mL) was added which caused the formation of a pale-yellow precipitate, which was filtered off, washed with THF (2×3 mL) and dried *in vacuo*. The desired product **5** (217.6 mg, 1.03 mmol, 64 %) was isolated as pale-yellow powder.

^{1}H-NMR (400 MHz, DMSO-d_6): δ(ppm) = 9.10 (*s*, 2 NH); 8.46 (*dd*, J = 4.4, 1.4 Hz, 2 arom. CH); 7.50 (*dd*, J = 8.1, 1.5 Hz, 2 arom. CH); 7.41 (*dd*, J = 8.1, 4.5 Hz, 2 arom. CH). ^{13}C-NMR (100 MHz, DMSO-d_6): δ(ppm) = 163.6 (1 C=O); 146.2 (2 arom. C_q); 145.7 (2 arom. CH); 137.8 (2 arom. C_q); 128.7 (2 arom. CH); 124.7 (2 arom. CH). FT-IR (neat) *ν*[cm^{-1}]: 3223*w* (*ν*N–H), 3098*w*, 2980*w*, 2936*w*, 1687*s* (*ν*C=O), 1578*m*, 1490*w*, 1461*m*, 1433*m*, 1402*m*, 1375*m*, 1321*w*, 1293*m*, 1229*m*, 1211*m*, 1115*w*, 1091*w*, 1064*m*, 896*m*, 834*s*, 738*m*, 808*m*, 738*m*, 718*m*, 642*w*, 617*s*, 572*m*, 486*m*. HR-ESI-MS: $[M+H]^+ = [C_{11}H_9ON_4]^+$; calc.: m/z 213.07709, found: m/z 213.07686 (−1.09 △ ppm).

5,7-Dihydro-6H-dipyrido[3,2-d:2′,3′-f][1,3]diazepine-6-thione (7)

Compound **3** (200.0 mg, 1.07 mmol, 1.0 eq.) was dissolved in degassed DMSO (3 mL). CS_2 (1 mL, 20.22 mmol, 18.8 eq.) was added and the reaction mixture was stirred at 100 °C for 4.5 h. A color change of the solution from yellow to red was observed. After UHPLC-MS indicated completion of reaction, the solvent was evaporated *in vacuo* and the brown crude product was resuspended in THF (3 mL). The pale beige solid was filtered off, washed with THF (3×3 mL) and dried *in vacuo*. The desired product **7** (253.0 mg, 0.57 mmol, quant.) was isolated as pale beige solid.

^{1}H-NMR (400 MHz, DMSO-d_6): δ(ppm) = 10.37 (*s*, 2 NH); 8.48 (*dd*, J = 4.4, 1.1 Hz, 2 arom. CH); 7.51 (*dd*, J = 8.1, 1.1 Hz, 2 arom. CH); 7.41 (*dd*, J = 8.1, 4.4 Hz, 2 arom. CH). ^{13}C-NMR (100 MHz, DMSO-d_6): δ(ppm) = 192.8 (1 C=S); 146.5 (2 arom. CH); 146.4 (2 arom. C_q); 138.2 (2 arom. C_q); 128.9 (2 arom. CH); 124.4 (2 arom. CH). FT-IR (neat) *ν*[cm^{-1}]: 3188*m* (*ν*N–H), 3060*m*, 3000*m*, 1619*m*, 1553*m*, 1464*m*, 1397*s*, 1283*m*, 1215*s*, 1144*s* (*ν*C=S), 1070*w*, 890*w*, 837*w*, 795*m*, 735*s*. HR-ESI-MS: $[M+H]^+ = [C_{11}H_9N_4S]^+$; calc.: m/z 229.05424, found: m/z 229.05419 (−0.22 △ ppm).

5-Methyl-6-(methylthio)-5H-dipyrido[3,2-d:2′,3′-f][1,3]diazepine (8)

A mixture of **13** (100.0 mg, 0.44 mmol, 1.0 eq.) and KOH (8.4 mg, 1.76 mmol, 4.0 eq.) in degassed DMSO was stirred at ambient temperature and MeI (90 µL, 1.44 mmol, 3.2 eq.) was added in 5 µL steps over 6.5 h, until UPLC-MS indicated completion of the reaction. The solvent was evaporated *in vacuo* and the brown crude product was suspended in 5 mL H_2O. The pale beige solid was filtered off, washed with H_2O (3×2 mL) and dried *in vacuo*. The desired product **8** (67.2 mg, 0.26 mmol, 59 %) was isolated as pale beige solid.

^{1}H-NMR (400 MHz, DMSO-d_6): δ(ppm) = 9.49–8.48 (*m*, 1 arom. CH); 8.46 (*dd*, J = 3.8, 2.1 Hz, 1 arom. CH); 7.65 (*dd*, J = 8.3, 1.0 Hz, 1 arom. CH); 7.48 (*dd*, J = 8.3, 4.5 Hz, 1 arom. CH); 7.42–7.41 (*m*, 2 arom. CH); 3.21 (*s*, 1 N–CH_3); 2.48 (*s*, 1 S–CH_3). ^{13}C-NMR (100 MHz, DMSO-d_6): δ(ppm) = 166.0 (1 C–S); 148.7 (1 arom. C_q); 148.3 (1 arom. C_q); 146.7 (1 arom. C_q); 146.3 (1 arom. CH); 145.7 (1 arom. CH); 144.4 (1 arom. C_q); 133.2 (1 arom. CH); 126.0 (1 arom. CH); 124.2 (1 arom. CH); 124,0 (1 arom. CH); 35.7 (1 N–CH_3) 15.0 (1 S–CH_3). FT-IR (neat) *ν*[cm^{-1}]: 2994*w*, 2918*w*, 1605*s* (*ν*C=N), 1594*w*, 1557*m*,

1456*w*, 1435*m*, 1418*s*, 1418*w*, 1298*m*, 1280*w*, 1223*w*, 1143*m*, 1113*w*, 1095 *s*, 1061 *s*, 1040 *s*, 978*w*, 858*w*, 848*w*, 813*s*, 764*w*, 742*s*, 658*m*, 623*w*, 606*m*, 499*m* HR-ESI-MS: $[M+H]^+ = [C_{13}H_{13}N_4S]+$; calc.: m/z 257.08554, found: m/z 257.08556 (+0.08 △ ppm).

Metal Complexes

General procedure for the preparation of *fac*-[Re(CO)$_3$(diimine)Br] complexes: $(NEt_4)_2[Re(CO)_3\ Br_3]$ (1.5 eq.) and the diimine chelators (1.0 eq.) were dissolved in degassed MeOH (5 mL) in a Schlenk round bottom flask equipped with a reflux condenser. The intensely colored solutions were refluxed at 70 °C for 3 h. Reaction progress was monitored by formation of colored precipitates or by UHPLC-MS. The crude reaction mixtures were cooled to room temperature after complete consumption of the bipyridyl chelators. The solids were collected by filtration and washed with ice cold MeOH (2×2 mL). After drying *in vacuo*, the desired complexes were isolated as yellow to red crystalline solids.

[Re(CO)$_3$(1)Br] (**9**)

$(NEt_4)_2[ReBr_3(CO)_3]$ (314.2 mg, 0.41 mmol, 2.5 eq.) and **1** (40.0 mg, 0.16 mmol, 1.0 eq.) gave 9 (60.0 mg, 0.10 mmol, 63 %) as a dark red solid.

^{1}H-NMR (400 MHz, $CDCl_3$): δ(ppm) = 9.33 (*dd*, *J* = 5.4, 1.3 Hz, 2 arom. CH); 8.81 (*dd*, 2 arom. CH); 7.96 (*dd*, *J* = 8.4, 5.4 Hz, 2 arom. CH). FT-IR (neat) *ν*[cm^{-1}]: 3091*w*, 2031*m* (*ν*C≡O), 1921*s* (*ν*C≡O), 1897*s* (*ν*C≡O), 1601*m*, 1537*s* (*ν*N=O), 1426*m*, 1347*m* (*ν*N=O), 1115*m*, 875*m*, 825*m*, 776*m*. Elemental Analysis: calc: 26.18 % C, 1.01 % H, 9.40 % N, found: 28.28 % C, 1.65 % H, 8.60 % N. HR-ESI-MS: $[M+Na]^+ = [C_{13}H_6BrN_4O_7ReNa]^+$; calc.: m/z 618.88696, found: m/z 618.88574 (−1.98△ ppm).

[Re(CO)$_3$(3)Br] (**10**)

$(NEt_4)_2[ReBr_3(CO)_3]$ (438.1 mg, 0.43 mmol, 1.5 eq.) and **3** (40.0 mg, 0.16 mmol, 1.0 eq.) gave **10** (56.9 mg, 0.29 mmol, 78 %) as a yellow solid.

^{1}H-NMR (400 MHz, MeOD): δ(ppm) = 8.95 (*dd*, *J* = 5.6, 1.3 Hz, 2 arom. CH); 7.85 (*dd*, *J* = 8.2, 1.3 Hz, 2 arom. CH); 7.58 (*dd*, *J* = 5.6, 8.2 Hz, 5.0 arom. CH). FT-IR (neat) *ν*[cm^{-1}]: 3266*w* (*ν*N–H), 3197*w* (*ν*N–H), 3128*w*, 3070*w*, 2925*w*, 2855*w*, 2363*w*, 2352*w*, 2030*s* (*ν*C≡O), 1900s (*ν*C≡O), 1699*w*, 1608*w*, 1583*w*, 1442*m*, 1283*w*, 1259*w*, 1214*w*, 1156*w*, 1081 *m*, 1041*w*, 805*m*. UV-Vis (DMF, 25 μM, ε in $M^{-1}\cdot cm^{-1}$): λ_{max} = 514 (1640) Phosphorescence emission (DMF, 25 μM, excitation at 336 nm): λ_{max} = 618 nm, τ = 0.9 ± 0.1 ns. Elemental Analysis: calc: 29.11 % C, 1.88 % H, 10.45 % N, found: 28.17 % C, 2.60 % H, 8.11 % N. HR-ESI-MS: $[M+NH_4]^+ = [C_{13}H_{10}O_3N_4Re]^+$; calc.: m/z 457.03049, found: m/z 457.03039 (−0.22 △ ppm). Spectroscopic data was in agreement with literature.[18]

[Re(CO)$_3$(2)Br] (**11**)

$(NEt_4)_2[Re(CO)_3Br_3]$ (447.2 mg, 0.57 mmol, 1.5 eq.) and **2** (50.0 mg, 0.4 mmol, 1.0 eq.) gave **[6]** (200.8 mg, 0.4 mmol, quant.) as an orange powder.

^{1}H-NMR (400 MHz, $CDCl_3$): δ(ppm) = 9.33 – 9.30(*m*, 2 arom. CH); 8.75 – 8.71(*m*, 2 arom. CH); 7.89 – 7.85(*dd*, J = 8.5, 5.0 Hz, 5.0 arom. CH). FT-IR (neat) *ν*[cm^{-1}]: 3070*w*, 2926*w*, 2024*m* (*ν*C≡O), 1901*s* (*ν*C≡O), 1858*s* (*ν*C≡O), 1568*m* (*ν*N=N), 1518*m*, 1425*m*, 1270*m*, 1157*m*, 1133*m*, 1079 *m*, 825*s*, (in agreement with[24]). UV-Vis (DMF 25 μM, ε in $M^{-1}\cdot cm^{-1}$): λ_{max} = 322 (6896), λ_{max} = 335 (7044), λ_{max} = 397 (4152). Fluorescence emission (DMF, 25 μM, excitation at 336 nm): λ_{max} = 452 nm, τ = 9.3 ± 0.1 ns. Elemental Analysis: calc: 29.33 % C, 1.14 % H, 10.53 % N, found: 29.51 % C, 1.38 % H, 10.32 % N. HR-ESI-MS: $[M+NH_4]+ = [C_{13}H_{10}N_5O_3ReBr]^+$; calc.: m/z 549.95190, found: m/z 549.95075 (−2.09 △ ppm).

[Re(CO)$_3$(5)Br] (**12**)

$(NEt_4)_2[ReBr_3(CO)_3]$ (272.3 mg, 0.35 mmol, 1.5 eq.) and **11** (50.0 mg, 0.24 mmol, 1.0 eq) gave **12** (91.8 mg, 0.16 mmol, 67 %) as an orange powder.

^{1}H-NMR (400 MHz, DMSO-d_6): δ(ppm) = 9.81 (*s*, 2 NH); 8.68 – 8.67 (“*dd*”, 2 arom. CH); 7.72 – 7.70 (“*dd*”, 2 arom. CH); 7.59 (*dd*, J = 8.2, 5.2 Hz, 2 arom. CH). ^{13}C-NMR (100 MHz, DMSO-d_6): *δ*(ppm) = 197.8 (2 C≡O); 190.1 (1 C≡O); 158.6 (1 C=O); 148.5 (2 arom. C_q); 144.9 (2 arom. C_q); 139.0 (2 arom. CH); 131.6 (2 arom. CH); 128.8 (2 arom. CH). FT-IR (neat) *ν*[cm^{-1}]: 3248*w* (*ν*N–H), 3150*w*, 3068*w*, 2022*m* (*ν*C≡O), 1901*s* (*ν*C≡O), 1857*m* (*ν*C≡O), 1712*s* (*ν*C=O), 1579*m*, 1470*m*, 1479*m*, 1443*w*, 1411*m*, 1333*w*, 1229*w*, 1200*w*, 811*m*, 767*w*, 659*w*, 659*w*, 643*w*, 481*w*. UV-Vis (DMF, 25 μM, ε in $M^{-1}\cdot cm^{-1}$): λ_{max} = 387 (8848). Phosphorescence emission (DMF, 25 μM, excitation at 389 nm): λ_{max} = 643 nm τ = 81.2 ± 1.3 ns. Elemental Analysis: calc: 29.90 % C, 1.43 % H, 9.96 % N, found: 28.39 % C, 1.58 % H, 9.75 % N. HR-ESI-MS: $[M-Br]^+ = [ReC_{14}H_8N_4O_4]^+$; calc.: m/z 483.00976, found: m/z 483.00946 (−0.61 △ ppm);

$[M-H]^- = [ReC_{11}H_9N_3O_7Br]^-$; calc.: m/z 560.91869, found: m/z 560.91916 (0.85 △ ppm).

$[Re(CO)_3(6)Br]$ (13)

Compound **5** (100 mg, 0.47 mmol, 1.0 eq.) was dissolved in degassed DMSO (3 mL) in a 25 mL Schlenk round bottom flask. KOH (79 mg, 1.41 mmol, 3.0 eq.) and MeI (117 µL, 1.88 mmol, 4.0 eq) was added in 5 µL steps over 2 h over 4.5 h (*Scheme 4*). UHPLC-MS reaction control showed full consumption of **6**. The solvent was removed under high vacuum. The resulting oil was purified via preparative HPLC (gradient: 20% MeOH for 3 min, 20% to 100% MeOH in 28 min, 100% MeOH for 10 min, detection at 280 nm). Fractions containing **6** were collected and lyophilized. A highly hygroscopic yellow powder was obtained which quickly became an oil. This product was directly used in the next step, where it was added to $(NEt_4)_2[Re(CO)_3Br_3]$ (100.0 mg, 97.3 mmol, 0.2 eq.) in degassed MeOH (3 mL). The reaction mixture was stirred and heated to 70 °C until UPLC-MS indicated completion of reaction after 3 h. Yellow precipitate had formed, which was filtered off and washed with MeOH (3×2 mL). The desired product **13** (47.8 mg, 0.08 mmol, 17% based on **5**) was isolated as yellow powder.

^{1}H-NMR (400 MHz, DMSO-d_6): δ(ppm) = 8.84 (*dd*, J = 5.0, 0.6 Hz, 2 arom. CH); 8.14 (*dd*, J = 8.6, 0.8 Hz, 2 arom. CH); 7.81 (*dd*, J = 8.6, 5.0 Hz, 2 arom. CH); 3.19 (*s*, 3 H, CH_3). ^{13}C-NMR (100 MHz, DMSO-d_6): δ(ppm) = 197.5 (2 C≡O); 189.9 (1 C≡O); 162.5 (1 C=O); 149.2 (2 arom. C_q); 148.6 (2 arom. C_q); 143.2 (2 arom. CH); 133.0 (2 arom. CH); 128.8 (2 arom. CH); 37.4 (2 N–CH_3). FT-IR (neat) *v*[cm^{-1}]: 3085*w*, 2022*m* (*v*C≡O), 1926*s* (*v*C≡O), 1882*s* (*v*C≡O), 1858*s* (*v*C≡O), 1691*s* (*v*C=O), 1571*m*, 1472*m*, 1442*m*, 1422*m*, 1325*s*, 1302*m*, 1193*m*, 1136*w*, 1098*w*, 1077*w*, 968*w*, 859*w*, 818*m*, 725*m*, 670*w*, 643*m*, 629*m*, 613*m*, 550*m*, 523*w*, 475*m*. UV-Vis (DMF, 25 µM, ε in $M^{-1}\cdot cm^{-1}$): 374 (8795). Phosphorescence emission (DMF, 25 µM, excitation at 398 nm): λ_{max} = 655 nm τ = 26.3 ± 0.1 ns. Elemental Analysis: calc: 32.55% C, 2.05% H, 9.49% N, found: 31.85% C, 2.17% H, 9.28% N. HR-ESI-MS: $[M-Br]^+ = [ReC_{16}H_{12}N_4O_4]^+$; calc.: m/z 511.04106, found: m/z 511.03962 (−2.81 △ ppm).

$[Re(CO)_3(8)Br]$ (14)

$(NEt_4)_2[Re(CO)_3Br_3]$ (120.2 mg, 0.15 mmol, 2.0 eq.) and **8** (20.0 mg, 0.08 mmol, 1.0 eq.) gave **14** (18.10 mg, 0.03 mmol, 38%) as a yellow powder.

^{1}H-NMR (500 MHz, THF-d_8): δ(ppm) = 8.71–8.72 (*m*, 2 arom. CH); 7.71–7.49 (*m*, 4 arom. CH); 3.34 (*s*, 3 H, N–CH_3); 2.55 (*s*, 3 H, S–CH_3). ^{13}C-NMR (126 MHz, THF-d_8): δ(ppm) = 197.7 (1 C≡O); 197.6 (1 C≡O); 190.0 (1 C≡O); 168.3 (1 C–S); 150.1 (1 arom. C_q); 149.8 (1 arom. CH); 149.0 (1 arom. C_q); 147.8 (1 arom. C_q); 146.9 (1 arom. CH); 146.8 (1 arom. CH); 138.5 (1 arom. CH); 131.0 (1 arom. CH); 129.3 (1 arom. CH); 128.6 (1 arom. CH); 36.9 (N–CH_3); 16.2 (S–CH_3). FT-IR (neat) *v*[cm^{-1}]: 3068*w*, 2024*m* (*v*C≡O), 1906*s* (*v*C≡O), 1896*s* (*v*C≡O), 1614*m* (*v*C=N), 1588*s*, 1556*m*, 1473*w*, 1442*s*, 1421*m*, 1308*m*, 1280*w*, 1123*w*, *1079w*, 1057 *m*, 805*m*, 783*m*, 723*m*, 643*m*, 629*w*, 542*w*, 525*w*, 505*w*, 490*m*, 466*w*. UV-Vis (THF, 25 µM, ε in $M^{-1}\cdot cm^{-1}$): λ_{max} = 224 (24425), λ_{sh} = 251 (17260), λ_{max} = 281 (15171), λ_{max} = 400 (4370). UV-Vis (DMF, 25 µM, ε in $M^{-1}\cdot cm^{-1}$): λ_{max} = 266 (20004), λ_{max} = 374 (8795). Fluorescence emission (DMF, 25 µM, excitation at 337 nm): λ_{max} = 456 nm τ = 1.7 ± 0.1 ns. Phosphorescence emission (THF, 25 µM, excitation at 402 nm): λ_{max} = 650 nm τ = 9.8 ± 0.1 ns. Elemental Analysis: calc: 31.69% C, 1.99% H, 9.24% N, found: 33.37% C, 4.58% H, 6.49% N. HR-ESI-MS: $[M-Br]^+ = [ReC_{16}H_{12}N_4O_4]^+$; calc.: m/z 527.01719, found: m/z 527.01821 (−1.95 △ ppm).

$[Re(CO)_3(4)Br]$ (15)

Preparation of **4** according to a literature procedure as presented in *Scheme 5*.[21] **3** (105 mg, 584 µmol, 1.0 eq) and ethyl benzimidate hydrochloride (115 mg, 620 µmol, 1.1 eq) were dissolved in degassed MeOH (25 mL) in a two necked round bottom flask equipped with a septum, reflux condenser and stir bar. The resulting yellow solution was heated to 80 °C for 3 h. A slight color change from yellow to orange occurred.

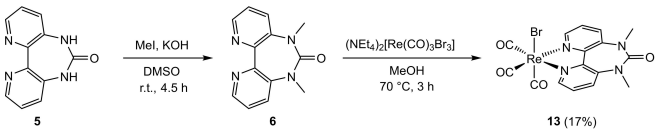

Scheme 4. Synthetic procedure going from **5** to **13** via the intermediate **6**.

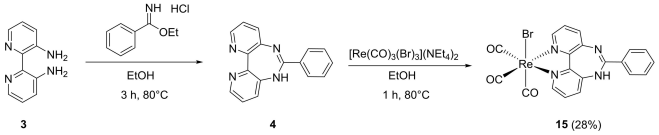

Scheme 5. Synthetic procedure going from **3** to **15** via the intermediate **4**.

Reaction progress was monitored by TLC (Alox, 9:1 CH_2Cl_2/MeOH) to check for the consumption of **3**. $[Re(CO)_3(Br)_3](NEt_4)_2$ (456 mg, 592 μmol, 1.05 eq) was suspended in 10 mL degassed EtOH and added to the reaction solution. An immediate color change from orange to red was observed. The reaction solution was stirred at 80 °C for 1 h. The reaction mixture was concentrated *in vacuo* to on third of the original volume. Addition of H_2O (10 mL) caused a red precipitate to form which was collected by centrifugation. The red solid was washed with H_2O (10 mL) and centrifuged. The title compound **15** (205 mg, 329 μmol, 58 %) was isolated as a deep red crystalline solid.

^{1}H-NMR (400 MHz, DMSO-d_6): δ(ppm) = 9.29 (*s*, 1 H, NH); 8.50–8.45 (*d* like *m*, 2 arom. CH); 7.92–7.87 (*d* like *m*, 2 arom. CH); 7.64 (*tt*, J = 7.5, 1.8 Hz, 1 arom. CH); 7.58–7.50 (*m*, 4 arom. CH); 7.49–7.43 (*m*, 2 arom. CH). ^{13}C-NMR (100 MHz, DMSO-d_6): δ(ppm) = 197.8 (2 C≡O); 190.0 (1 C≡O); 161.0; 150.7; 149.8; 148.9; 148.6; 147.9; 145.8; 140.5; 134.8; 132.8; 131.5; 129.6; 129.4; 129.3; 128.8. FT-IR (neat) *v*[cm^{-1}]: 3274*w*, 3245*w*, 2020*s* (*v*C≡O), 1899*s* (*v*C≡O), 1650*m*, 1566*w*, 1450*m*, 1415*m*, 1316*w*, 1237*w*, 1117*w*, 805*w*, 692*w*, 645*w*. UV-Vis (DMF, 25 μM, ε in $M^{-1}\cdot cm^{-1}$): λ_{max} = 362 (8916), λ_{max} = 487 (3351), Fluorescence emission (DMF, 25 μM, excitation at 420 nm): λ_{max} = 501, λ_{max} = 541 nm, τ (not assigned) = 1.5 ± 0.1 and 5.1 ± 0.1 ns. Phosphorescence emission (DMF, 25 μM, excitation at 420 nm): λ_{max} = 609, τ = 23.4 ± 3.8 ns. Elemental Analysis: calc: 37.84 % C, 2.45 % H, 8.51 % N, found: 37.84 % C, 2.74 % H, 8.02 % N. HR-ESI-MS: $[M-H]^- = [C_{20}H_{11}BrN_4O_3Re]^-$; calc.: m/z 620.95775, found: m/z 620.95685 (−1.46 △ ppm).

$(NEt_4)[(Re(CO)_3Br)\mu_2\text{-}7(Re(CO)_3Br_2)]$ (NEt_4[16])

$(NEt_4)_2[ReBr_3(CO)_3]$ (135.0 mg, 0.17 mmol, 2.0 eq.) and **7** (20.0 mg, 0.08 mmol, 1.0 eq.) gave NEt_4**[16]**) (56.8 mg, 0.05 mmol, 57 %) as a dark orange powder.

^{1}H-NMR (400 MHz, DMSO): δ(ppm) = 10.81 (*s*, 2 NH); 8.63 (*dd*, J = 1.0, 5.2 Hz, 2 arom. CH); 7.73 (*dd*, J = 1.0, 8.4 Hz, 2 arom. CH); 7.55 (*dd*, J = 5.2, 8.4 Hz, 2 arom. CH); 3.20 (*dd*, J = 7.2, 14.5 Hz, 4 CH_2); 1.17 (*tt*, J = 1.8, 3.6, 7.2 Hz, 4 CH_3). ^{13}C NMR (100 MHz, DMSO): δ(ppm) = 197.7 (C≡O); 189.8 (C≡O); 187.0 (C=S); 149.3 (2 arom. C); 146.0 (2 arom. C); 138.7 (2 arom. C); 132.2 (2 arom. C); 129.1 (2 arom. C); 51.8 (4 CH_2, NEt_4); 7.6 (4 CH_3, NEt_4). FT-IR (neat) *v*[cm^{-1}]: 3183*w* (N–H), 3004*w*, 2022*m* (*v*C≡O), 2009*m* (*v*C≡O), 1910*s* (*v*C≡O), 1892*s* (*v*C≡O), 1872*s* (*v*C≡O), 1866*s* (*v*C≡O), 1630*m*, 1572*m*, 1472*m*, 1406*m*, 1415*m*, 1317*m*, 1220*w*, 1186*w*, 1146*m* (*v*C=S), 1139*w*, 999*w*, 801*m*, 725*w*, 714*w*. UV-Vis (DMF, 25 μM, ε in $M^{-1}\cdot cm^{-1}$): λ_{max} = 293 (26143), λ_{max} = 412 (7863). Phosphorescence emission: (DMF, 25 μM, excitation at 358 nm): λ_{max} = 662 nm, τ = 73.7 ± 0.7 ns. Elemental Analysis: calc: 26.37 % C, 2.48 % H, 6.15 % N, found: 24.94 % C, 2.31 % H, 5.98 % N. HR-ESI-MS: $[M-NEt_4-HBr]^- = [Re_2C_{17}H_7N_4Br_2O_6S]^-$; calc.: m/z 926.75736, found: m/z 926.75417 (−3.44 △ ppm).

$[Re(CO)_3(bpy)Br]$

$(NEt_4)_2[ReBr_3(CO)_3]$ (110.9 mg, 144 μmol, 1.5 eq.) and bipyridine (15 mg, 96 μmol, 1.0 eq) gave $[Re(CO)_3(bpy)Br]$: (44 mg, 87 μmol, 91 %) as an orange powder.

Spectroscopic data matches literature.[32] ^{1}H-NMR (400 MHz, DMSO): δ(ppm) = 9.03–9.02 (*"dd"*, 2 arom. CH); 8.75–8.74 (*"dd"*, 2 arom. CH); 8.32 (*dt*, J = 15.8, 8.0, 1.4 Hz, 2 arom. CH); 7.76–7.74 (*"dt"*, 2 arom. CH). ^{13}C NMR (100 MHz,DMSO): δ(ppm) = 197.8 (2 C≡O); 189.9 (1 C≡O); 155.6 (2 arom. C_q); 153.6 (2 arom. CH); 140.7 (2 arom. CH); 128.3 (2 arom. CH); 124.8 (2 arom. CH). FT-IR (neat) *v*[cm^{-1}]: 3081*w*, 2009*m* (*v*C≡O), 1879*s* (*v*C≡O), 1603*w*, 1469*w*, 1442*w*, 1313*w*, 1246*w*, 1155*w*, 1119*w*, 1105*w*, 1072*w*, 1044*w*, 1011*w*, 768*s*, 760*m*, 645*m*, 627*m*, 534*m*, 489*m*, 464*m* (in agreement with[26]). UV-Vis (THF, 25 μM, ε in $M^{-1}\cdot cm^{-1}$): λ_{max} = 210 (35463), λ_{sh} = 240 (23863), λ_{max} = 295 (20255), λ_{max} = 394 (3456). UV-Vis (DMF, 25 μM, ε in $M^{-1}\cdot cm^{-1}$): λ_{max} = 293 (15823), λ_{sh} = 317 (9866), λ_{max} = 375 (3290). Phosphorescence emission (DMF, 25 μM, excitation at 376 nm): λ_{max} = 620 nm, τ = 49.3 ± 0.2 ns. Elemental Analysis: calc: 26.37 % C, 2.48 % H, 6.15 % N, 2.82 % S, found: 24.94 % C, 2.31 % H, 5.98 % N, 2.91 % S. HR-ESI-MS: $[M-Br]^+ = [ReC_{13}H_8N_2O_3]^+$; calc.: m/z 427.00869, found: m/z 427.00806 (−1.48 △ ppm).

Supporting Information

Deposition Number(s) 2310845 (for **7**), 2310846 (for **8**), 2310847 (for **11**), 2310848 (for **12**), 2310849 (for **13**), 2310850 (for **14**), 2310857 (for **15**), 2310851 (for NEt_4**[16]**) contain(s) the supplementary crystallographic data for this paper. These data are provided free of charge by the joint Cambridge Crystallographic Data Centre and Fachinformationszentrum Karlsruhe Access Structures service. Detailed crystallographic data is also available in the *Supporting Information*

available free of charge on the WWW under https://doi.org/10.1002/hlca.202300239;. The authors have cited additional references within the *Supporting Information*.[20,23,27,33–37]

Author Contribution Statement

J.C. rote the manuscript and supervised experiments. N.D. and S.J. performed the synthetic and analytical work of the compounds reported herein. O.B. and B.S. performed crystallographic work. RA conceived the project and organized funding for the project.

Acknowledgements

We acknowledge the support of the MS, NMR and X-ray facilities at the University of Zurich. Open Access funding provided by Universität Zürich.

Data Availability Statement

The data that support the findings of this study are available in the supplementary material of this article.

References

[1] S. Bullock, A. J. Hallett, L. P. Harding, J. J. Higginson, S. A. F. Piela, S. J. A. Pope, C. R. Rice, 'Luminescent rhenium fac-tricarbonyl-containing complexes of androgenic oxo-steroids', *Dalton Trans.* **2012**, *41*, 14690–14696.

[2] B. Probst, A. Rodenberg, M. Guttentag, P. Hamm, R. Alberto, 'A Highly Stable Rhenium-Cobalt System for Photocatalytic H_2 Production: Unraveling the Performance-Limiting Steps', *Inorg. Chem.* **2010**, *49*, 6453–6460.

[3] M. Oberholzer, B. Probst, D. Bernasconi, B. Spingler, R. Alberto, 'Photosensitizing Properties of Alkynylrhenium(I) Complexes $[Re(-C\equiv C-R)(CO)_3(N\cap N)]$ ($N\cap N$ = 2,2′-bipy, phen) for H_2 Production', *Eur. J. Inorg. Chem.* **2014**, *2014*, 3002–3009.

[4] M. Mosberger, B. Probst, B. Spingler, R. Alberto, 'Influence of Hetero-Biaryl Ligands on the Photo-Electrochemical Properties of $[ReINCS(N\cap N)(CO)_3]$-Type Photosensitizers', *Eur. J. Inorg. Chem.* **2019**, *2019*, 3518–3525.

[5] C. Bachmann, B. Probst, M. Guttentag, R. Alberto, 'Ascorbate as an electron relay between an irreversible electron donor and Ru(ii) or Re(i) photosensitizers', *Chem. Commun.* **2014**, *50*, 6737–6739.

[6] W. Hieber, R. Schuh, H. Fuchs, 'Über Metallcarbonyle. XXXVII. Über Rhenium-halogeno-pentacarbonyle, ihre Bildungstendenz und Eigenschaften', *ZAAC* **1941**, *248*, 243–255.

[7] E. W. Abel, G. Wilkinson, '291. Carbonyl halides of manganese and some related compounds', *J. Chem. Soc.* **1959**, 1501–1505.

[8] M. Wrighton, D. L. Morse, 'Nature of the lowest excited state in tricarbonylchloro-1,10-phenanthrolinerhenium(I) and related complexes', *J. Am. Chem. Soc.* **1974**, *96*, 998–1003.

[9] P. J. Giordano, S. M. Fredericks, M. S. Wrighton, D. L. Morse, 'Simultaneous multiple emissions from fac-XRe $(CO)_3$(3-benzoylpyridine)$_2$: n-. pi.* intraligand and charge-transfer emission at low temperature', *J. Am. Chem. Soc.* **1978**, *100*, 2257–2259.

[10] B. Probst, PhD Thesis thesis, University of Zurich (Zürich), 2010.

[11] Y. Liang, M. T. Nguyen, B. J. Holliday, R. A. Jones, 'Electrocatalytic reduction of CO_2 using rhenium complexes with dipyrido[3,2-a:2,3-c]phenazine ligands', *Inorg. Chem. Commun.* **2017**, *84*, 113–117.

[12] J. Hawecker, J.-M. Lehn, R. Ziessel, 'Electrocatalytic reduction of carbon dioxide mediated by Re(bipy)(CO)3Cl (bipy = 2,2-bipyridine)', *J. Chem. Soc. Chem. Commun.* **1984**, 328–330.

[13] L. Rotundo, D. C. Grills, R. Gobetto, E. Priola, C. Nervi, D. E. Polyansky, E. Fujita, 'Photochemical CO_2 Reduction Using Rhenium(I) Tricarbonyl Complexes with Bipyridyl-Type Ligands with and without Second Coordination Sphere Effects', *ChemPhotoChem* **2021**, *5*, 526–537.

[14] J. Hawecker, J.-M. Lehn, R. Ziessel, 'Efficient photochemical reduction of CO_2 to CO by visible light irradiation of systems containing $Re(bipy)(CO)_3X$ or $Ru(bipy)_3^{2+}$–Co^{2+} combinations as homogeneous catalysts', *J. Chem. Soc. Chem. Commun.* **1983**, 536–538.

[15] A. Maurin, C.-O. Ng, L. Chen, T.-C. Lau, M. Robert, C.-C. Ko, 'Photochemical and electrochemical catalytic reduction of CO_2 with NHC-containing dicarbonyl rhenium(i) bipyridine complexes', *Dalton Trans.* **2016**, *45*, 14524–14529.

[16] J. Hawecker, J.-M. Lehn, R. Ziessel, 'Photochemical and Electrochemical Reduction of Carbon Dioxide to Carbon Monoxide Mediated by (2,2-Bipyridine)tricarbonylchlororhenium(I) and Related Complexes as Homogeneous Catalysts', *Helv. Chim. Acta* **1986**, *69*, 1990–2012.

[17] K. Schindler, F. Zobi, 'Photochemistry of Rhenium(I) Diimine Tricarbonyl Complexes in Biological Applications', *Chimia* **2021**, *75*, 837.

[18] F. L. Thorp-Greenwood, J. A. Platts, M. P. Coogan, 'Experimental and theoretical characterisation of phosphorescence from rhenium polypyridyl tricarbonyl complexes', *Polyhedron* **2014**, *67*, 505–512.

[19] B. Probst, M. Guttentag, A. Rodenberg, P. Hamm, R. Alberto, 'Photocatalytic H2 Production from Water with Rhenium and Cobalt Complexes', *Inorg. Chem.* **2011**, *50*, 3404–3412.

[20] S. Kanoktanaporn, J. A. H. MacBride, 'Preparation of ring-fused pyridazines by reduction of 3,3-dinitro-4,4-bipyridyl and 3,3-dinitro-4,4-biquinolyl', *J. Chem. Soc.-Perkin Trans.* **1978**, 1126–1131.

[21] K. Matsuda, I. Yanagisawa, Y. Isomura, T. Mase, T. Shibanuma, 'Alternative Synthesis of Dibenzo-and Dipyrido-[1,3]Diazepines from Thioamides and o,o'-Diaminobiaryls', *Synth. Commun.* **1997**, *27*, 2393–2402.

[22] J. K. Hino, L. Della Ciana, W. J. Dressick, B. P. Sullivan, 'Substituent constant correlations as predictors of spectroscopic, electrochemical, and photophysical properties in ring-substituted 2,2′-bipyridine complexes of rhenium(I)', *Inorg. Chem.* **1992**, *31*, 1072–1080.
[23] C. R. Rice, S. Onions, N. Vidal, J. D. Wallis, M.-C. Senna, M. Pilkington, H. Stoeckli-Evans, 'The Coordination Chemistry of 3,3-Diamino-2,2-bipyridine and Its Dication: Exploring the Role of the Amino Groups by X-ray Crystallography', *Eur. J. Inorg. Chem.* **2002**, *2002*, 1985–1997.
[24] S. Stoyanov, I. Petkov, L. Antonov, T. Stoyanova, P. Karagiannidis, P. Aslanidis, 'Thione-thiol tautomerism and stability of 2- and 4-mercaptopyridines and 2-mercaptopyrimidines', *Can. J. Chem.* **1990**, *68*, 1482–1489.
[25] A. E. S. Fairfull, D. A. Peak, W. F. Short, T. I. Watkins, '918. Some derivatives of 1:6-diazapyrene and 4:5–6:7-dibenzo-1:3-diazacyclohepta-2:4:6-triene', *J. Chem. Soc.* **1952**, 4700–4709.
[26] P. Kurz, PhD Thesis, University of Zurich **2005**.
[27] L. Farrugia, 'ORTEP-3 for Windows – a version of ORTEP-III with a Graphical User Interface (GUI)', *J. Appl. Crystallogr.* **1997**, *30*, 565.
[28] R. Bolliger, A. Frei, H. Braband, G. Meola, B. Spingler, R. Alberto, 'Chemistry at High Dilution: Dinuclear 99mTc Complexes', *Chem. Eur. J.* **2019**, *25*, 7101–7104.
[29] M. J. Stout, B. W. Skelton, A. N. Sobolev, P. Raiteri, M. Massi, P. V. Simpson, 'Synthesis and Photochemical Properties of Re(I) Tricarbonyl Complexes Bound to Thione and Thiazol-2-ylidene Ligands', *Organometallics* **2020**, *39*, 3202–3211.
[30] F. Zobi, B. Spingler, R. Alberto, 'Guanine and Plasmid DNA binding of Mono- and Trinuclear fac-$[Re(CO)_3]^+$ Complexes with Amino Acid Ligands', *ChemBioChem* **2005**, *6*, 1397–1405.
[31] L. Kaczmarek, P. Nantka-Namirski, A. Kłodzińska, B. Bujak, E. Tatarczyńska, 'Synthesis and pharmacological properties of some dipyrido[1,3]diazepinones', *Pol. J. Pharmacol. Pharm.* **1991**, *43*, 387–393.
[32] G. Albertin, S. Antoniutti, J. Castro, S. García-Fontán, G. Schipilliti, 'Preparation and Reactivity of Hydridorhenium Complexes with Polypyridine and Phosphonite Ligands', *Eur. J. Inorg. Chem.* **2007**, *2007*, 1713–1722.
[33] R. C. Clark, J. S. Reid, 'The analytical calculation of absorption in multifaceted crystals', *Acta Crystallogr. Sect. A* **1995**, *51*, 887–897.
[34] R. O. D. L. CrysAlisPro (version 1.171.42.57a), Yarnton, Oxfordshire, England, 2022.
[35] G. Sheldrick, 'SHELXT – Integrated space-group and crystal-structure determination', *Acta Crystallogr. Sect. A* **2015**, *71*, 3–8.
[36] A. Spek, 'Structure validation in chemical crystallography', *Acta Crystallogr. Sect. D* **2009**, *65*, 148–155.
[37] G. Sheldrick, 'Crystal structure refinement with SHELXL', *Acta Crystallogr. Sect. C* **2015**, *71*, 3–8.

Received December 19, 2023
Accepted January 9, 2024

